马　凯[1, 2]，　孙大千[1]，　宣兆志[1]，　陆　佳[1]

（1.　　　　　　　　　　　　　，　　　　　130022；2.　　　　　　　　　　，　　　　　130012）

：　　　　　　　　　　　　　　　　　　　　，

　　　　　　　　　AZ91D　　　　　　　，　　　　　。

　　　　　　　，　　　　　　　　，

。　　　　　　　　，

，　　　　　，　　　　　　50 nm

，　　　　　　　　。

：　　　；　　　；　　　；

马　凯

0　序　言

　　　　　　　　　　　　　　，
　　　、
　　　　　　　　　，
[1, 2]，　　　　、　　　、
、　、
。　，　　　　　　　，
　　　　　　　　　　。

　　　　　　、　　　、　　、　　、
　　、　　　、　　　、　　　、
[3]。　　　　　　　　　　　　Al
　　，　　　　　　　　　　
[4]
。

　　　　　　　，　　[5]
　　　Al　　　　　　　　，
[6]　　　　　　　　　　Al
　　　。

，　　　　Al　　　，
　　，
。

1　试验方法

　　　　　AZ91D　　　　　，

3 mm，　　≥99.5%　　。
　　　XDP-1　　　　　　；JSM-5600LV
　　　；D/Max 2500Pc　X　　　　　；JEM-
2000EX　　　　　　；YWX/Q-0160　　　；
GX71　　　　　。

　　　70 mm×40 mm×8 mm　　　　，
　　　　　。

　　　　　　180 A，
100 mm，　　　　　　，
　　　　。

　　　10 mm×10 mm×8
mm　　　　；　　，
SEM，XRD　TEM　　。

2　试验结果及分析

2.1
2.1.1　电弧电压对涂层微观组织的影响
　　　1　　　　　（　　　30 V，
0.6 MPa）　　　。　2　0.6 MPa
，　　　26 V　33 V
。　1　　　，
：　　　，
，
，
，
。　　　　2b　33 V，

，

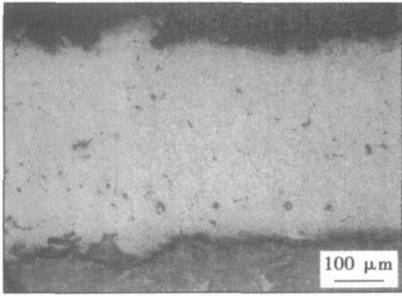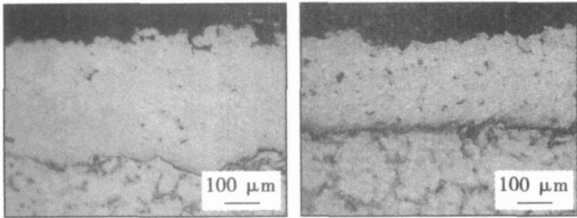，   。

1   30 V

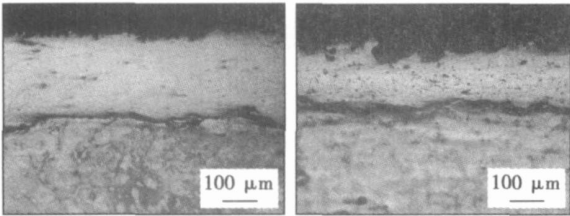Fig. 1   Microstructure of coating at voltage 30 V

(a) 电压 26 V   (b) 电压 33 V

2   26 V   33 V

Fig. 2   Microstructure of coatings at voltages of 26 V and 33 V

2.1.2   喷涂气压对涂层微观组织的影响

3   30 V   0.5 MPa   0.7 MPa

。   ，

1   。   :   ，

，   ，   ，

。   ，   ，   ，   ，
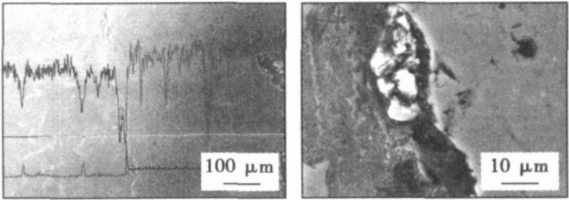
，   。   ，

，   。

(a) 气压 0.5 MPa   (b) 气压 0.7 MPa

3

Fig. 3   Microstructure of coatings at different spray air pressure

2.1.3   涂层与基体界面组织分析

4   。

4a   ，

，

，   Mg

，   Al   ，

，Al   ，

，   、   ，

，Mg   ，

，

。

(a) 涂层与基体界面的线扫描像 (b) 涂层与基体界面的微观放大像

4

Fig. 4   Line scan and SEM photography in boundary area of coating and matrix

4b   ，

。   Mg–Al

$Mg_{17}Al_{12}$[7]。   :   ，

，   ，

，   ，

，

。 $Mg_{17}Al_{12}$

，   ，   。

2.1.4   涂层断口形貌分析

5   SEM   。   ，

，

，   。

，   ，

5
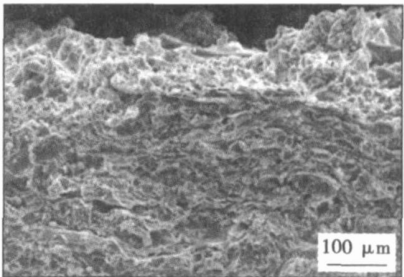
Fig. 5   Fracture morphology of coating

，

，　　　　　　　　　　　　　　　。

2.1.5　涂层的 XRD 分析

　　　　6　　　X　　　　。　　　　4

Al　，　　　　　　　　　　　，

　　　　　　　Al　，　　　　　　　　　。

　　　　　，　　　　　　　　　　　。

　　　：　　　　　　　　　　　　，

　　　　，　　　　　　　　　　　，

　。　　　，　　　　　　　　　　　，

6　　　　　　X
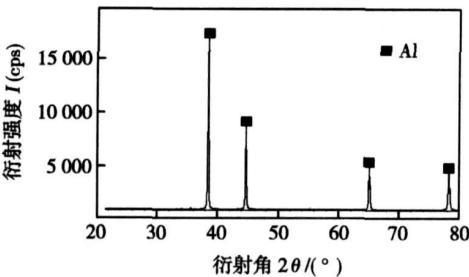
Fig. 6　XRD spectra of coating

2.1.6　涂层相结构分析

　　　　7　　　　　　　　。　　　7a　　，

　　　　　　　，　　　　　100 ~ 200 nm

，　　　　　　　　　　50 nm

　　　　　。　　　　7b

　　　　。　　　　　　　　，

　　　　　　，

　　　。　　　7b　　　　，

7a　　　　　　Al　　。

7
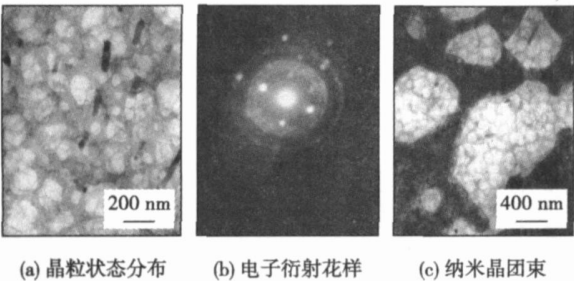
Fig. 7　Transmission and local electron diffraction photography
of coating

7c

　　　　　　　　　　　　　　　，

　　　　　　　　　：　　　　　　，

　　　　　　　，　　　　　　，

，　　　　，　　　　。

2.2

2.2.1　电极电位测定

　　　　　　　，　　　　，

　，　　　　　，

5 % NaCl　　　，　　　25 ℃,　　0.01 V/min,

−2.0 ~ 0.0 V。　8　　　　　Tafel

（E-lg I　　, lg I　　　　　　　）。

　　，　　　（　）　　，

（　）　　　，　　　，

AB　，　　−1.0 ~ −0.76 V

，　　　　　，

　　。　　　　　，

　　，

8
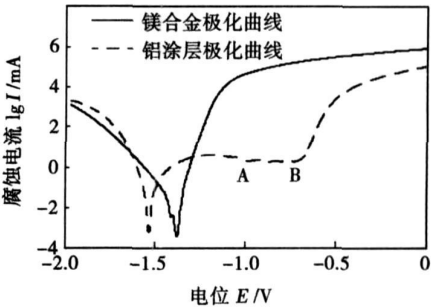
Fig. 8　Tafel polarization curve

2.2.2　涂层孔隙率测定

　　　　　　　，

　　　　，　　　　　　　。

　　　，　　　　，

[8]。　　1　　　　　180 A,

100 mm

　　　。　1　，30 V　，0.6 MPa

，　5.09 %,

。

2.2.3　中性盐雾试验

GB6458 − 86,

。　　　　pH

6.8　5 % NaCl　　，　　　，

1

Table 1　Porosity of coating

	U/V	p/MPa	$\eta/\%$
1	33	0.6	7.18
2	30	0.6	5.09
3	26	0.6	12.15
4	23	0.6	22.88
5	30	0.7	9.34
6	30	0.5	15.01

48 h。　　　　　　，　　1 h　，
　　35%

，　　　　　　　　　　　　　　　　　　。
4 h　，　　　　　　　　　　　　　　　　，
　　　，　　　　　　　　　　　　。　　　9
48 h　　。　　　　　　　　（　9a）
　　　，　　　　　　（　9b）　　，
　　　。　，　　　　48 h
，　　　　　　　　　，

，　　　　　，

。
，　　　　48 h　　　　　　。
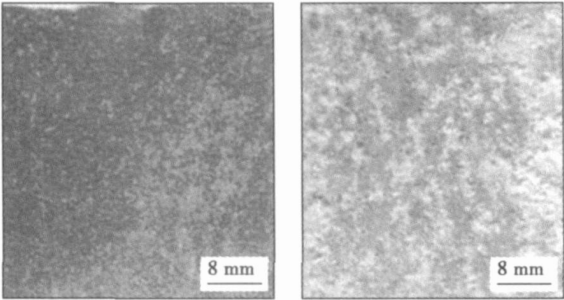
(a) 基材表面48 h腐蚀状况　　(b) 涂层表面48 h腐蚀状况

9

Fig. 9　Salt-spray corrosion contrast between base metal and coating

3　结　　论

（1）　　　　　　30 V，　　　　　　0.6 MPa
　　　　　　　　。
（2）　　　　　　　　，
　　Mg17Al12，
　　　　　。
（3）　　　　　　　　　　　　。

　　　　　　：

[1] M F Montemor, A M Simes, M J Carmezim. Characterization of rare-earth conversion films formed on the AZ31 magnesium alloy and its relation with corrosion protection[J] . Applied Surface Science, 2007, 253; 6922—6931.

[2] Li W, Zhou H, Zhou W, et al. Effect of cooling rate on ignition point of AZ91D 0.98 wt.% Ce magnesium alloy [J] . Materials Letters, 2007(61); 2772—2774.

[3] 　　　，　　，　　　，　. 　　　　　　　　[M] . 　：
　　　, 2007.

[4] 　　，　. AZ91D
　[J] . 　　, 2006 35(6); 17—18.

[5] 　. 　　　　　　　　　　[J] .
　　, 2007, 28(2); 102—105.

[6] 　，　，　，　. 　　　AZ91D
　[J] . 　　, 2005, 29(3); 29—31.

[7] 　. 　　　　　　[J] . 　, 2002
(3); 66—69.

[8] Crotty D, Stinecker C, Durkin B. Plating difficult substrates with electroless Nickel [M] . Cincinnati, USA; Gardner Publications, Inc. 1996.

　　　　：　　，　，1968　　　，　　　，　　。
　　　　　　。　　　　10

Email：basan780@sohu.com

Finite element analysis of residual stress of welding repair for gas pipeline

YANG Linjuan[1, 2], SHEN Shiming[1] (1. College of Mechanical and Power Engineering, Nanjing University of Technology, Nanjing 210009, China; 2. Science and Technology Administration Office, Nantong Vocational College, Nantong 226007, China). p77—80

Abstract: By the finite element analysis software ABAQUS and the function of coupling process between heat and stress, the methods of entirety welding repair and local welding repair were simulated for 20-steel gas pipeline, and the distributions of the two kinds of welding residual stress were obtained. At the same time, the stress of welding-repair joint was analyzed by ABAQUS under inner pressure and welding residual stress. The results indicate that the residual stress of the entirety welding repair is lower than that of the local welding repair. And under inner pressure and welding residual stress, the tensile stress of the entirety welding repair is lower than that of the local welding repair too. It shows that the entirety welding repair joint is stronger than the local welding repair joint. The method of the entirety welding repair can reduce the probability of stress corrosion cracking and fit for the engineering application. The research results provide theory base for optimizing welding repair technology.

Key words: gas pipeline; entirety welding repair; local welding repair; welding residual stress; finite element analysis

Temperature control system of electron beam brazing joint

WANG Xuedong, LIU Peng, WANG Wei (Department of Mechanical Engineering, Tsinghua University, Beijing 100084, China). p81—84

Abstract: High precision digital PID control system used in temperature control of electron beam brazing joint was realized. In order to keep the predefined joint temperature during brazing process, digital control model and controller were constructed based on computer control and discrete control theories. The type of the controlled object was determined by open-loop and closed-loop step responses, and the effect of the expanded ultimate-sensitivity method and the expanded step-response method were compared when the PID parameters were tuning. The PID parameters obtained by the ultimate-sensitivity method were optimized by the through normalization on line, and each group of parameters and the corresponding experimental results were provided. Integration separation algorithm was also used to enhance the dynamic performances. The experimental results show that overshoot is so small that can be ignored and time is not needed to adjust; the temperature control precision can reach $\pm$ 2.5 ℃.

Key words: electron beam brazing; closed-loop control; discrete control system

Effects of trace indium on properties and microstructure of Ag-Cu-Zn filler metal

LU Fangyan[1], XUE Songbai[1], ZHANG liang[1], LAI Zhongmin[1, 2], GU Liyong[3], GU Wenhua[3] (1. Nanjing University of Aeronautics and Astronautics, Nanjing 210016, China; 2. Jiangsu University of Science and Technology, Zhenjiang 212003,

China; 3. Changshu Huayin Filler Metals Co. Ltd., Changshu 215513, China). p85—88

Abstract: Melting temperature, spreadability, microstructures of silver filler metal bearing different content of indium, and the mechanical properties of brazed joints were studied respectively. By using copper and brass plates as base metal, brazing with flame method, the mechanical properties of the joints brazed with lap-joint and butt joint were tested and analyzed at the same time. Results show that adding indium can decrease the melting temperature and improve the spreadability of the silver filler metal, and the microstructures of the silver filler metal bearing different content of indium are refined significantly. For the lap-joint of brass, the tensile strength of the joints gradually strengthens, presenting parabolic shape, with the increasing of the element indium; the fractures position of two kinds of brazed joints happens on the base metal, except for the lap-joint of brass, which shows better mechanical properties of the joints brazed with the silver filler metals bearing indium.

Key words: silver filler metal; melting temperature; spreadability; mechanical properties; microstructure

Microstructure and interface analysis of aluminum coating sprayed by electro-arc spraying on AZ91D magnesium alloy

MA Kai[1, 2], SUN Daqian[1], XUAN Zhaozhi[1], LU Jia[1] (1. School of Materials Science and Engineering, Jilin University, Changchun 130022, China; 2. School of Mechanical and Electrical Engineering, Changchun Institute of Technology, Changchun 130012, China). p89—92

Abstract: In order to obtain the excellent composite coating on magnesium alloy, double aluminum wires as two electrodes were automatically fed to create electric arc, the melting aluminum drops were sprayed on the AZ91D magnesium alloy surface by compressed air, and then the Mg-Al composite coating was formed. The optimum processing parameters were found by selecting different voltages and air pressure to carry on the spray experiments and analyzing the influence of the parameters on the coating structure performance. The characteristics of the coating microstructure and interface were researched by using the modern analysis methods, and the coating corrosion resistance was analyzed by test the coating electrode potential and the salt-spray experiment. The results indicate that certain voltage and air pressure can cause the coating to be compact. There is the newborn microstructure in the interface. The dual-structures of nano-scale crystal beam and micron-scale lamellar under 50 nm appear in the coating. The corrosion resistance of the coating surpasses that of the magnesium alloy matrix obviously.

Key words: magnesium alloy; arc spray aluminium; nano-crystalline; corrosion resistance

Effects of heat treatment technology on mechanical properties of friction welding drill rod

ZHU Hai[1], ZHENG Haiyang[2], GUO Yanling[1] (1. Mechanical and Electrical Engineering College, Northeast Forest University, Harbin 150040, China; 2. Drilling Tool Subcompany of Daqing Drilling Technology Services Company, Daqing 163461, China). p93—96